

Efficient and Accurate Calibration to FX Market Skew with Fully Parameterized Local Volatility Model

Dongli Wu, Bufan Zhang, Xiao Lin¹

CCB Fintech
Shanghai 200120, China

ABSTRACT: When trading American and Asian options in the FX derivatives market, banks must calculate prices using a complex mathematical model. It is often observed that different models produce varying prices for the same exotic option, which violates the non-arbitrage requirement of derivative risk management. To address this issue, we have studied a fully parameterized local volatility model for pricing American/Asian options. This model, when implemented using a grid or Monte-Carlo numerical method, can be efficiently and accurately calibrated to FX market skew volatilities. As a result, the model can provide reliable prices for exotic options during daily trading activities.

KEY WORDS: FX derivatives pricing, American option, Asian option, local volatility model.

1 Introduction

Recently, the China Foreign Exchange Trade System (CFETS) opened two types of FX exotic derivatives business in the interbank market: American options and Asian options. Unlike European options, which are traded by prices quoted in the liquid market, banks must issue prices for exotic options by calculating them using complicated mathematical models. A review paper by Homescu [1] provides a list of such models. It is a common requirement for banks and financial institutions that a mathematical model for pricing FX derivatives

¹E-mail: xiao_lin_99@qq.com; First version: 2022-11-15; This version: 2023-04-21.

should be arbitrage-free in a risk-neutral market. However, in daily banking practice, it is often observed that different models produce different prices even for a specific exotic option.

To eliminate arbitrage opportunities, it is common practice in the financial industry to calibrate the model before pricing FX derivatives. The formulation for such calibration can be found in the paper by Derman and Kani [2]. Calibration is often the most difficult task in model development, particularly when the model has a complex mathematical structure and many free parameters. Calibration is also essential for model validation, as the model's performance during calibration provides a unique standard for judging an arbitrage-free model. Unfortunately, despite a vast number of existing publications, such as [1-7], it is difficult to find a model that efficiently and accurately calibrates to the FX market skew volatility surface.

The purpose of this paper is to study a fully parameterized local volatility model (LV) for efficient and accurate volatility calibration. This LV model delivers satisfactory pricing for our trading desk.

In Section 2, we briefly describe the deal structure for FX American and FX Asian options. The values of these options depend on the evolution of FX market prices throughout the entire life of the deals. Therefore, a model that takes into account the evolution process of FX prices and volatilities is necessary for pricing.

Section 3 presents the mathematical formulation of the fully parameterized local volatility model. The stochastic differential equation is similar to that of a log-normal model, but the volatility is a function of time and the underlying FX price. When performing numerical calculations, the volatility function can be discretized using a set of two-dimensional parameters. It is important to choose a sufficiently large number of parameters to accurately calibrate to the market.

In Section 4, we present a grid numerical method for solving the stochastic LV model equation. This method is most efficient for pricing American options, where the deal value is independent of the historical path of the market FX price.

In Section 5, we present a Monte-Carlo numerical method for solving the stochastic LV model equation. This method is most suitable for pricing Asian options, where the deal value strongly depends on the historical path of the market FX price.

In Section 6, we focus on model calibration. We formulate a mathematical procedure using the Levenberg-Marquardt method to calibrate the LV model parameters. With an example, we show that this procedure can efficiently and accurately calibrate the model parameters for the full FX market volatility matrix. We also provide two conditions for the input market volatility data necessary for successful calibration.

In Section 7, we present two calculation examples to demonstrate the pricing accuracy of American and Asian options using the LV model. We show that the LV model in this paper produces prices that quickly converge to stability when increasing the number of grids or Monte-Carlo paths, and that errors are stable within 1 basis point. This satisfies trading requirements.

Finally, in Section 8, we compare our one-factor LV model to the two-factor LSV (Local-Stochastic Volatility) model, which is currently widely used in the financial industry. Since the LV model in this paper performs exceptionally well in both model calibration and pricing, we suggest that there is no need to extend this model to the two-factor LSV model.

2 Deal structure of American/Asian options

First, we briefly review the deal structure of two types of exotic options.

The American option is an extension of the European option. In the traditional European option, the option buyer has the right (but not the liability) to buy or sell a certain amount of foreign currency N at a previously determined unit price K on the expiration date T_e . In the corresponding American option, the exercise date is not restricted to T_e only, but falls within a time period. For example, in the USDCNY option market, a bank buys an American call option today, $t_0 = 20221012$. The bank has one opportunity to buy USD 1000000 using the price $K = 7.1234$ during the time period from $T_s = 20221112$ to $T_e = 20231012$. Let $S(t)$ be the FX price of USDCNY at time t . When the option is exercised, the immediate profit in CNY to the bank is

$$\text{Payoff}(t) = N \max(S(t) - K, 0). \quad (1)$$

The American option requires a human action to be exercised. If the bank does not exercise the option during the time period $T_s \leq t \leq T_e$, its value becomes zero.

An Asian option has a common expiration date T_e like a European option. However, their payoffs are calculated differently. Let $T_s \leq t^1 < t^2 < \dots < t^n \leq T_e$ be a time series in the option lifetime. The time series can be set up in several ways, for example, daily, weekly, or monthly, but all t^k must be a CFETS working date so that there is always an FX rate $S^k = S(t^k)$, ($k = 1, 2, \dots, n$) available for calculating the payoffs. Let

$$\begin{aligned}\bar{S} &= \frac{1}{n}(S^1 + S^2 + \dots + S^n), \\ \hat{S} &= \left(S^1 S^2 \dots S^n\right)^{\frac{1}{n}}.\end{aligned}\tag{2}$$

There are four types of payoffs in Asian options. Taking the call option as an example, the first is called Arithmetic Spot (all in CNY)

$$\text{Payoff}(T_e) = N \max(\bar{S} - K, 0).\tag{3}$$

The second is called Geometric Spot

$$\text{Payoff}(T_e) = N \max(\hat{S} - K, 0).\tag{4}$$

The third is called Arithmetic Strike

$$\text{Payoff}(T_e) = N \max(S(T_e) - \bar{S}, 0).\tag{5}$$

The last is called Geometric Strike

$$\text{Payoff}(T_e) = N \max(S(T_e) - \hat{S}, 0).\tag{6}$$

In general, if $t^n < T_e$, there may be $S(T_e) \neq S_n$.

3 Fully parameterized local volatility model

As the payoffs of American or Asian options depend on the evolution process of the FX rate $S(t)$ over a future time period $T_s \leq t \leq T_e$, we require a stochastic model to formulate the changes of $S(t)$.

Assuming that $S(t)$ in $0 < t \leq T_e$ is governed by a local volatility process:

$$\frac{dS}{S} = \mu dt + \sigma(t, S) dw,\tag{7}$$

Table 1: Fully parameterized local volatility function $\sigma(t, s)/100$.

day/s	0.0	0.1	0.2	0.3	0.4	0.5	0.6	...	1.0
0.0	4.300	4.300	4.300	4.300	4.300	7.746	4.300	...	4.300
1.0	4.303	4.376	3.950	3.190	2.449	5.150	2.449	...	4.317
2.5	4.299	4.292	4.322	3.947	2.630	0.828	2.630	...	4.301
4.0	4.299	4.207	3.842	3.535	2.353	0.218	2.353	...	4.315
9.0	4.309	4.308	3.726	2.681	3.266	3.054	3.266	...	4.336
14.0	4.315	4.528	4.234	3.244	3.833	3.374	3.833	...	4.363
17.5	4.309	4.515	4.885	4.396	3.679	3.775	3.679	...	4.343
21.0	4.309	4.741	5.978	6.007	4.991	5.540	4.991	...	4.356
25.5	4.301	4.610	6.211	6.686	6.227	5.987	6.227	...	4.318
30.0	4.310	4.344	4.954	3.995	2.646	2.803	2.646	...	4.334
59.0	4.324	4.892	5.252	4.943	4.983	5.132	5.382	...	4.455
91.0	4.282	4.324	5.675	5.333	4.329	4.422	4.098	...	4.338
179.0	4.290	4.204	3.783	3.902	3.763	3.124	4.156	...	4.552
273.0	4.291	4.121	4.214	4.761	4.628	3.896	4.098	...	4.462
365.0	4.293	4.240	3.823	4.021	4.199	3.393	4.214	...	4.524
547.0	4.293	4.167	4.125	4.854	4.751	3.773	4.336	...	4.446
730.0	4.298	4.233	3.629	3.830	3.911	3.255	4.485	...	4.469
1094.0	4.298	4.254	3.976	5.202	5.454	3.303	4.859	...	4.362

Here, $\mu = \mu(t)$ is the deterministic drift term, $w = w(t)$ is a Brownian motion, and $\sigma(t, S)$ is the volatility (also called model volatility to distinguish it from market volatility in the following). This model is called a local volatility model because $\sigma(t, S)$ is a function of time t and the local FX state $S = S(t)$. From equation (7), as long as the function $\sigma(t, S)$ is known, we can solve the stochastic process for $S(t)$.

We can discretize the continuous function $\sigma(t, S)$ by a set of two-dimensional parameters. First, we perform a variable transformation for S as follows:

$$s = \Phi\left(\frac{\ln(S/F_t)}{1.3c_0\sqrt{t + 1/365.25}}\right), \quad (8)$$

where F_t is the forward FX value at time t (which can be obtained from the FX curve), c_0 is a constant that can be set to the 1-year ATM market volatility, and $\Phi(\cdot)$ is the cumulative

probability function of the normal distribution:

$$\Phi(x) = \frac{1}{\sqrt{2\pi}} \int_{-\infty}^x e^{-\frac{1}{2}y^2} dy. \quad (9)$$

Using the variable s , we can restrict the definition domain of $\sigma(t, S)$ to a rectangular region:

$$0 \leq t \leq T_e, \quad 0 \leq s \leq 1. \quad (10)$$

This region can be divided into a set of small rectangular elements, in which the function is calculated using bilinear interpolation. As an example, Table 1 shows a discrete volatility surface $\sigma(t, s)$ that has been decomposed into 18×11 grids. The number of grids can be increased if the computer's memory and speed improve.

4 Grid method for American options

The value of an American option at time $t = T$ is independent of the historical path of the underlying $S(t)$ in $t < T$. Therefore, a grid method can be used to evaluate the American option. To price thousands of deals for the desk, we need to build a symmetric, stable, and flexible grid. In the grid method, we will first ignore the drift term. The work is carried out based on the following model equation:

$$dx = \sigma(t, S)dw, \quad S = e^{x+\mu}, \quad (11)$$

where $\mu = \mu(t)$ is a parameter for curve calibration to the FX forward curve.

If a correct volatility function $\sigma(t, S)$ is already known, the entire pricing process in the grid method can be divided into three stages: grid setup, curve calibration by forward propagation, and deal valuation by backward propagation. However, if the correct volatility function $\sigma(t, S)$ is not yet available, we assume a volatility function and use the three-stage process repeatedly to calibrate the volatility until we have the correct volatility function. After that, we can perform the valuation work. In this section, we focus on the three-stage process by assuming that the correct volatility function is available. The volatility calibration is discussed in Section 6.

The grid setup in the first stage includes both a time grid and a state grid.

We begin by setting up the time grid, which divides the time period t ($0 < t < T_e$) into several small intervals. The process starts by collecting special dates (e.g., expiration dates) from market volatility instruments and American option deals to be priced. These dates form the initial time series. If an interval in the initial time series is too large (for example, greater than 3 days), we add more dates in between to create a finer-grained grid. This completes the time grid setup.

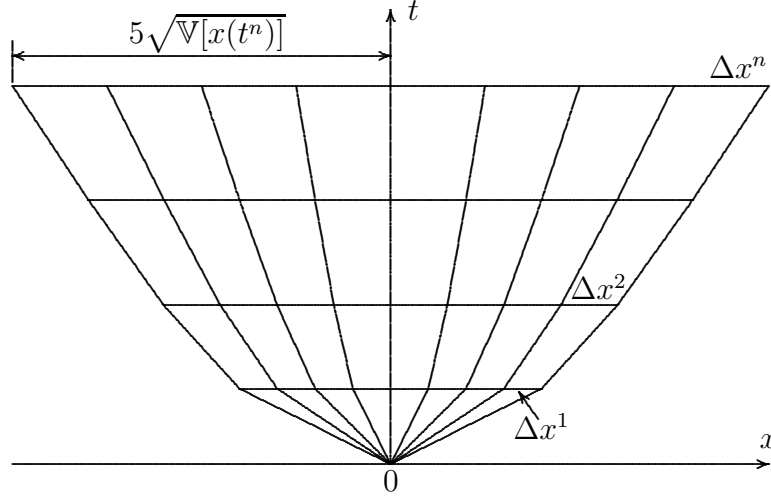


Figure 1: A tree-like grid field.

Then we set up the state grid. We denote the time series as $t^0 = 0, t^1, t^2, \dots$. We build a tree-like grid field, similar to the one shown in Figure 1. The half-space width at date t is set to 5 times the standard deviation of $x(t)$, which can be calculated using the variance in the following formula,

$$\mathbb{V}[x(t^n)] = \mathbb{V}[x(t^{n-1})] + \sigma_{\max}^2 \Delta t, \quad (12)$$

where, $\sigma_{\max} = \max_{t=t^n} \{\sigma(t, S(t))\}$. The half space width is divided into a number of I intervals Δx^n (for example, $I \geq 50$). Then, there are a total of $2I + 1$ state grid points at time t^n ,

$$x_i^n = 5\sqrt{\mathbb{V}[x(t^n)]} \frac{i}{I}, \quad (i = 0, \pm 1, \pm 2, \dots, \pm I). \quad (13)$$

Each grid point x_i^n is mapped to an FX state, namely

$$S_i^n = \exp(x_i^n + \mu^n). \quad (14)$$

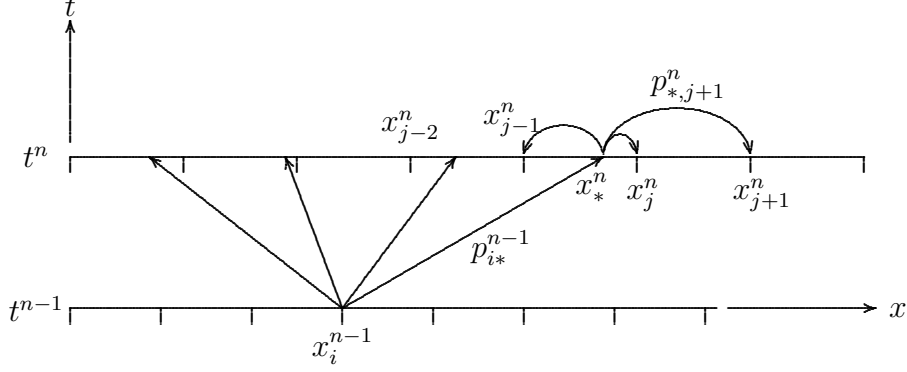


Figure 2: Transition probability between grid points.

We still need to determine the transition probability in the grid setup. We use p_{ij}^{nl} to denote the transition probability from point x_i^n to x_j^l . In case that $l = n + 1$, we will omit the l and simply write it as p_{ij}^n . Then, the transition probability from grid point x_i^{n-1} to x_j^n , namely p_{ij}^{n-1} , is calculated in two steps, as shown in Figure 2.

In the first step, a quaternary tree is created to the starting point x_i^{n-1} by

$$\begin{aligned} \Delta w &= \left(-\sqrt{3\Delta t}, -\sqrt{\frac{\Delta t}{3}}, \sqrt{\frac{\Delta t}{3}}, \sqrt{3\Delta t} \right), \\ p_{i*}^{n-1} &= \left(\frac{1}{8}, \frac{3}{8}, \frac{3}{8}, \frac{1}{8} \right). \end{aligned} \quad (15)$$

Each tree branch points to one of the four intermediate points x_*^n at time t^n , namely

$$x_*^n = x_i^{n-1} + \sigma(t^{n-1}, S_i^{n-1}) \cdot \Delta w. \quad (16)$$

In the second step, for each intermediate point x_*^n , we find a grid point x_j^n that is closest to it. From a Taylor expansion, we can calculate a state variable S_*^n at point x_*^n by combining three neighboring values, as follows:

$$S_*^n = \frac{1}{2}(\xi^2 - \xi) S_{j-1}^n + (1 - \xi^2) S_j^n + \frac{1}{2}(\xi^2 + \xi) S_{j+1}^n, \quad (17)$$

where $\xi = (x_*^n - x_j^n)/\Delta x^n$. The coefficients in the formula can be referred to as the transition probabilities from x_*^n to the three neighboring grid points, namely,

$$p_{*,j-1}^{nn} = \frac{1}{2}(\xi^2 - \xi), \quad p_{*,j}^{nn} = (1 - \xi^2), \quad p_{*,j+1}^{nn} = \frac{1}{2}(\xi^2 + \xi). \quad (18)$$

Thus, the transaction probability from the grid point x_i^{n-1} to grid point x_j^n is obtained by a train rule that combines equations (15) and (18), as follows:

$$p_{ij}^{n-1} = \sum_{*} p_{i*}^{n-1} \cdot p_{*j}^{nn}. \quad (19)$$

The parameter μ^n in (14) needs to be determined in order to map the grid point x_i^n to an FX state $S_j^n = \exp(x_j^n + \mu^n)$ and calculate the volatility $\sigma_j^n = \sigma(t^n, S_j^n)$. This process is called curve calibration. We begin the process at $t = t^0 = 0$, with only one state $S(x_0^0 + \mu^0)$ at the root grid x_0^0 . Let this state be equal to the FX spot $F(t^0)$ published at t^0 .

$$S_0^0 = S(x_0^0 + \mu^0) = e^{x_0^0 + \mu^0} = F(t^0), \quad (20)$$

we determine μ^0 .

According to the previous assumption that the local volatility function $\sigma = \sigma(t, S)$ is ready, we can calculate the volatility $\sigma(t^0, S_0^0)$ and transition probability p_{0k}^0 . Denote the arriving probability at point x_k^n by $q_k^n = p_{0k}^{0n}$. It can be seen that $q_k^1 = p_{0k}^0$. Thus, the parameter μ^1 can be determined by letting the expectation of the state FX at time t^1 be equal to the FX spot published at the same date t^1 , namely,

$$\sum_{k=-I}^I p_{0k}^0 S_k^1 = \sum_{k=-I}^I q_k^1 S(x_k^1 + \mu^1) = F(t^1). \quad (21)$$

With $S_k^1 = S(x_k^1 + \mu^1)$, we have the volatility $\sigma(t^1, S_k^1)$ and the transition probability p_{kj}^1 . Then, the probability of reaching the grid x_j^2 can be computed using the transition probability rule.

$$q_j^2 = \sum_{k=-I}^I p_{0k}^0 p_{kj}^1 = \sum_{k=-I}^I q_k^1 p_{kj}^1 \quad (22)$$

Let the expectation of the FX state at date t^2 be equal to the FX spot published at the same date t^2 , namely

$$\sum_{j=-I}^I q_j^2 S_j^2 = \sum_{j=-I}^I q_j^2 S(x_j^2 + \mu^2) = F(t^2). \quad (23)$$

We obtain μ^2 , as well as the grid state $S_j^2 = S(x_j^2 + \mu^2)$ at time t^2 for $j = -I, \dots, I$.

We continue this process to calculate μ^3, μ^4 , and so on until we reach the final time $t = T_e$. Then, we will finish the curve calibration and have the whole grid states $S_i^n = S(t^n, S_i)$, which can be used to calculate the value of American options.

The above calculation for grid states is called *forward propagation*. Once completed, a grid field $\{x_k^n\}$ is built. Each grid is mapped to an FX state $S_k^n = S(x_k^n + \mu^n)$, with which the option value can be calculated. For example, for a call option, if x_j^{n+1} is a grid at the final time step of expiration date $t^{n+1} = T_e$, the option value is calculated by

$$V_j^{n+1} = \max(S_j^{n+1} - K, 0). \quad (24)$$

We are now moving back a step to another grid point x_k^n at date t^n . Given that the transition probability p_{kj}^n is known, the option values V_j^{n+1} can be expressed as the following \hat{V}_k^n from the viewpoint at x_k^n

$$\hat{V}_k^n = \exp(-r^n \Delta t) \sum_{j=-I}^I p_{kj}^n V_j^{n+1}, \quad (25)$$

where, $r^n = r(t^n)$ is the interest rate of currency 2 (CNY) at date t^n , and \hat{V}_k^n represents the option value if it is held on x_k^n and exercised on a future date $t > t^n$. If the option is exercised on x_k^n at t^n , the immediate payoff is $\max(S_k^n - K, 0)$. To exercise the option now, this payoff must be greater than the future value \hat{V}_k^n . Otherwise, it is preferable to keep the option for the future. Thus, the option value at the grid point x_k^n is the maximum of the current exercise value $\max(S_k^n - K, 0)$ and the future exercise value \hat{V}_k^n , namely

$$V_k^n = \max(S_k^n - K, \hat{V}_k^n). \quad (26)$$

It can be seen that equation (26) is equivalent to equation (24) except that we are now standing on the date t^n . We can use the process described in equation (25) by changing n to $n - 1$, and move the option value one step back to the date t^{n-1} . By repeating this process, we can propagate the option values of all grids back to the root grid x_0^0 and obtain the option PV, namely V_0^0 . This calculation process is called *backward propagation*.

The forward propagation and backward propagation calculation method described above was proposed by Bill Krasker from Salomon Brothers in the 1990s. It is an explicit method and has first-order precision for Δt and second-order precision for Δx . The Krasker method can be compared favorably to the Godunov method [8] in fluid dynamics because they both have a clear physical background, fast computation speed, high numerical precision, and strong working stability. They are also easy to code. Additionally, the Krasker method can be applied to two- or three-dimensional grid computations.

5 Monte-Carlo method for Asian options

The value of an Asian option at time $t = T$ depends on the historical path of the underlying $S(t)$ in $t < T$. Therefore, a Monte Carlo method is used to price the Asian option. Unlike the grid method, where a symmetric grid setup benefits the computation of the transition probability, there is no need for symmetry in the Monte Carlo paths. Thus, the work is carried out based on the following model equation,

$$\begin{aligned} dx &= -\frac{1}{2}\sigma^2(t, S)dt + \sigma(t, S)dw, \\ S(t + dt) &= S(t)e^{dx+\mu}, \end{aligned} \tag{27}$$

where $\mu = \mu(t)$ is a parameter for curve calibration to the FX forward curve.

Similar to the grid method, if a correct volatility function $\sigma(t, S)$ is already known, the Monte-Carlo pricing process can be divided into three stages: path generation, curve calibration by forward propagation, and deal valuation. If the correct volatility function $\sigma(t, S)$ is not available, an approximate volatility function will be assumed, and the three-stage process will be used repeatedly to calibrate the volatility until the correct function is obtained. Once the correct function is obtained, the valuation work can begin. This section focuses on the three-stage process assuming the correct volatility function is available. The volatility calibration is addressed in Section 6.

In the first stage of path generation, we set up both the time step and path state.

We start with the time step, in which the date period ($0 \leq t \leq T_e$) is divided into several small intervals. The work begins with collecting the expiration dates from market volatility instruments and the FX fixing dates from Asian option deals. These dates will form an initial time series. If an interval in the initial time series is too large (for example, greater than 3 days), we will add more dates in between.

Then, we move on to the path state. Suppose we prepare a number of I paths in the pricing, all of which have a common time series t^0, t^1, t^2, \dots . In the i -th path at date $t = t^n$, we take a random number ξ_i^n from normal distribution for the Browning motion dw in (27),

$$S_i^{n+1} = S_i^n \exp \left(-\frac{1}{2}\sigma^2(t^n, S_i^n)\Delta t + \sigma(t^n, S_i^n)\sqrt{\Delta t}\xi_i^n + \mu^n \right). \tag{28}$$

Thus we have a formula to generate the FX state paths for pricing.

The parameter μ^n in (28) needs to be determined to ensure that the state S_j^{n+1} is correct and to calculate the volatility $\sigma_j^{n+1} = \sigma(t^{n+1}, S_j^{n+1})$ at the next date t^{n+1} . This task is called curve calibration and must be done in conjunction with path generation. Starting from $n = 0$, all initial states S_i^0 of every path i must be equal to the FX spot published on t^0 ,

$$S_i^0 = F(t^0), \quad (i = 1, 2, \dots, I). \quad (29)$$

Suppose at date t^n we already have the correct states S_i^n and volatilities $\sigma_i^n = \sigma(t^n, S_i^n)$ for all paths $i = 1, 2, \dots, I$. We then project a test state at t^{n+1} for each path i by

$$\begin{aligned} X_i^{n+1} &= S_i^n \exp \left(-\frac{1}{2} \sigma^2(t^n, S_i^n) \Delta t + \sigma(t^n, S_i^n) \sqrt{\Delta t} \xi_i^n \right), \\ (i &= 1, 2, \dots, I). \end{aligned} \quad (30)$$

The non-arbitrage condition requires that the expectation of S_i^{n+1} be equal to the FX spot published on t^{n+1} , namely $F(t^{n+1})$. To satisfy this condition, let $\lambda = e^\mu$, and use the following parameter λ^{n+1} ,

$$\lambda^{n+1} = F(t^{n+1}) \left(\frac{1}{I} \sum_{i=1}^I X_i^{n+1} \right)^{-1}, \quad (31)$$

we obtain the non-arbitrage states at date t^{n+1} as follows,

$$S_i^{n+1} = \lambda^{n+1} X_i^{n+1}, \quad (i = 0, 1, \dots, I). \quad (32)$$

By repeating this work for $n + 2$, $n + 3$, and so on, we can complete curve calibration.

After calibrating the curve, we can begin valuing the Asian option deal. Along a given path i , we have FX states S_i^n at every date t^n where $n = 0, 1, 2, \dots$. We can calculate the average FX fixing using (2). The payoff of the option deal along this path i can be obtained using (3)-(6). By taking an average of the payoff over all paths and discounting it from the payment date back to t^0 , we obtain the deal present value (PV).

6 Volatility calibration

In order to perform the volatility calibration, we require an FX option pricer. The pricer can be constructed using either the grid method, as described in Section 4, or the Monte Carlo method, as described in Section 5.

Table 2: USDCNY Volatility Instruments on Valuation Date 20220926.

Vol	10D Put	25D Put	ATMF	25D Call	10D Call	ExpDate	PayDate
1 Day	-----	-----	6.4460	-----	-----	20220927	20220929
1 Week	-----	4.2750	4.2000	4.2750	-----	20220930	20221011
2 Week	3.4805	3.3375	3.2500	3.3375	3.7305	20221010	20221012
3 Week	3.8281	3.6855	3.5980	3.6855	4.0781	20221017	20221019
1 Month	4.3355	4.1810	4.0560	4.1810	4.5855	20221026	20221028
2 Month	4.3397	4.1644	4.1130	4.3144	4.6897	20221124	20221128
3 Month	4.6009	4.4779	4.4500	4.7279	5.1009	20221226	20221228
6 Month	4.5013	4.4060	4.3500	4.7560	5.2013	20230324	20230328
9 Month	4.3574	4.3344	4.3000	4.7344	5.5274	20230626	20230628
1 Year	4.3114	4.3238	4.3000	4.7488	5.3114	20230926	20230928
18 Month	4.2841	4.3260	4.3000	4.8010	5.3341	20240326	20240328
2 Year	4.2533	4.2909	4.3000	4.8409	5.3533	20240925	20240927
3 Year	4.2536	4.3420	4.3000	4.8920	5.3536	20250924	20250926

Suppose there are n free parameters in the local volatility surface $\sigma(t, S)$. In the example of Table 1, $n = 198$, since there are 18 maturities (day) and 11 states (s), resulting in $18 \times 11 = 198$ free parameters. we represent these free parameters by a vector, namely

$$\mathbf{x} = (x_1, x_2, \dots, x_n)^T. \quad (33)$$

Suppose there are m market volatility instruments available. In this example, $m = 59$, as shown in Table 2. For the **1 Day** expiration tenor, we select only the at-the-money forward **ATMF** instrument, as the liquidity for out-of-the-money trades becomes very low within one business day. Similarly, for the **1 Week** tenor, we choose three out of five available instruments. The forward FX curve and CNY discount factor curve used for the calculation are shown in Table 3.

Each instrument is a European call or put option with a given delta (or strike). Therefore, for each instrument, we can calculate a price using the Black-Scholes formula, given the forward FX curve and discount factor curve. Let c_i , ($i = 1, 2, \dots, m$) be the price of the i -th instrument from the Black-Scholes formula (referred to as Market Price below). For the same i -th instrument, if a local volatility surface \mathbf{x} is given, we can also calculate a price using the grid method or Monte-Carlo method. We call this price the Model Price and denote it by

Table 3: USDCNY Forward FX Curve and CNY Discount Factor Curve on 20220926.

Days	Date	FX	Days	Date	Disc Factor	Zero Rate
0	20220926	7.091767	0	20220926	1	0
1	20220927	7.091267	1	20220927	0.99997030643729	1.084573480510
2	20220928	7.09055	92	20221227	0.99594227324328	1.614238917762
3	20220929	7.0903125	182	20230327	0.99127367379894	1.758944368042
15	20211011	7.0888775	274	20230627	0.98596080974996	1.884726241507
16	20221012	7.08729	366	20230927	0.98005664202941	2.010363044324
23	20221919	7.085325	732	20240927	0.95528848515717	2.282408600332
32	20221028	7.08319	1097	20250927	0.92834798649655	2.475463763546
63	20221128	7.075425	1826	20270926	0.86914126651663	2.805376130443
93	20221228	7.0664	3653	20320926	0.72952589429167	3.153172511253
183	20230328	7.04005				
275	20230628	7.02575				
367	20230928	7.007				
549	20240328	7.00455				
732	20240927	7.0013				
1096	20250926	7.03305				
1459	20260924	7.07605				
1824	20270924	7.01055				

$y_i = y_i(\mathbf{x})$, ($i = 1, 2, \dots, m$). We define a vector function by

$$\mathbf{f}(\mathbf{x}) = \left(\frac{y_1(\mathbf{x})}{c_1} - 1, \frac{y_2(\mathbf{x})}{c_2} - 1, \dots, \frac{y_m(\mathbf{x})}{c_m} - 1 \right)^T. \quad (34)$$

The objective of model calibration is to find a solution $\mathbf{x} = \hat{\mathbf{x}}$ for the equation

$$\mathbf{f}(\mathbf{x}) = \mathbf{0}. \quad (35)$$

The solution may not exist since (35) represents a non-linear function of \mathbf{x} . In general, the objective is to find a local minimum point $\mathbf{x} = \hat{\mathbf{x}}$ such that

$$\|\mathbf{f}(\hat{\mathbf{x}})\|^2 = \mathbf{f}^T(\hat{\mathbf{x}}) \cdot \mathbf{f}(\hat{\mathbf{x}}) = \text{minimum}. \quad (36)$$

We use the Levenberg-Marquardt method to solve (35). The starting point of this method is the Newton method. Let \mathbf{x}_k be an initial value of free parameters that we choose arbitrarily. We take a Taylor expansion for $\mathbf{f}(\mathbf{x})$ in (35) and obtain

$$\mathbf{f}(\mathbf{x}) = \mathbf{f}(\mathbf{x}_k) + \mathbf{A}(\mathbf{x}_k)(\mathbf{x} - \mathbf{x}_k) = \mathbf{0}, \quad (37)$$

where $\mathbf{A}(\mathbf{x}_k)$ is the Jacobian matrix defined as

$$\mathbf{A}(\mathbf{x}_k) = \frac{\partial \mathbf{f}(\mathbf{x}_k)}{\partial \mathbf{x}^T}, \quad (38)$$

and the partial derivatives in the formulas are calculated numerically using finite difference perturbation. From (37) we obtain an iteration formula for calculating the root

$$\mathbf{x}_{k+1} = \mathbf{x}_k - (\mathbf{A}^T \mathbf{A})^{-1} \mathbf{A}^T \mathbf{f}(\mathbf{x}_k). \quad (39)$$

If the iteration converges, the error will become smaller and smaller, namely,

$$\mathbf{f}^T(\mathbf{x}_{k+1}) \cdot \mathbf{f}(\mathbf{x}_{k+1}) \leq \mathbf{f}^T(\mathbf{x}_k) \cdot \mathbf{f}(\mathbf{x}_k). \quad (40)$$

However, the matrix $(\mathbf{A}^T \mathbf{A})$ may not be invertible, which can cause the iteration to fail. Even if the matrix is invertible, the moving step $(\mathbf{x}_{k+1} - \mathbf{x}_k)$ obtained by (39) may be too large to control the iteration process. Therefore, we can use the Levenberg-Marquardt method to perform the task. Let $\mathbf{w} = \mathbf{x} - \mathbf{x}_k$, and $\mathbf{f}_k = \mathbf{f}(\mathbf{x}_k)$. We can rewrite the (37) into another form,

$$\mathbf{A} \mathbf{w} = -\mathbf{f}_k. \quad (41)$$

Multiplying this equation by \mathbf{A}^T , and adding a diagonal element α , yields

$$(\mathbf{A}^T \mathbf{A} + \alpha \mathbf{I}) \mathbf{w} = -\mathbf{A}^T \mathbf{f}_k + \alpha \mathbf{w}. \quad (42)$$

In the Levenberg-Marquardt method, we first select a sufficiently large positive number α to ensure that the matrix $(\mathbf{A}^T \mathbf{A} + \alpha \mathbf{I})$ is positive-definite. We then solve the equation

$$(\mathbf{A}^T \mathbf{A} + \alpha \mathbf{I}) \mathbf{w} = -\mathbf{A}^T \mathbf{f}_k \quad (43)$$

for a solution \mathbf{w} . At this time, we perform two checks. The first check is to verify whether \mathbf{w} is still in the gradient direction of the original equation, namely,

$$\mathbf{w}^T \cdot (-\mathbf{A}^T \mathbf{f}_k + \alpha \mathbf{w}) > 0. \quad (44)$$

The second check is whether \mathbf{w} reduces the error, namely,

$$\mathbf{f}^T(\mathbf{x}_k + \mathbf{w}) \cdot \mathbf{f}(\mathbf{x}_k + \mathbf{w}) \leq \mathbf{f}^T(\mathbf{x}_k) \cdot \mathbf{f}(\mathbf{x}_k). \quad (45)$$

If both conditions are met, \mathbf{w} is valid. We will use $\mathbf{x}_{k+1} = \mathbf{x}_k + \mathbf{w}$ as the new initial condition for the next iteration, and decrease α by half. If at least one condition fails, we double α and test again until we find a valid \mathbf{w} . After several cycles of iterations, if $\|\mathbf{f}(\mathbf{x}_{k+1})\|$ decreases to 0, we get the exact solution $\hat{\mathbf{x}} = \mathbf{x}_{k+1}$. Otherwise, if $\|\mathbf{w}\| = \|\mathbf{x} - \mathbf{x}_k\|$ becomes very small, we also get an optimizing solution \mathbf{x}_{k+1} . Thus, the volatility calibration is finished.

Table 4 shows a result of the volatility calibration, where the error of each instrument is defined as

$$\text{Error}_i = f_i = \frac{y_i(\mathbf{x})}{c_i} - 1, \quad (i = 1, 2, \dots, m), \quad (46)$$

and the average calibration error is

$$\text{AvgError} = \sqrt{\frac{1}{m} \mathbf{f}^T(\mathbf{x}) \cdot \mathbf{f}(\mathbf{x})} = \sqrt{\frac{1}{m} \sum_{i=1}^m \left(\frac{y_i(\mathbf{x})}{c_i} - 1 \right)^2} = 0.0003. \quad (47)$$

The above volatility calibration was performed using the grid method. We found that the accuracy of the calibration depends mainly on the smoothness of the market instrument volatility surface (Table 2). For this calibration data, the result is equally good if the Monte-Carlo method is used. However, for unrealistic/arbitrageable market volatilities, the calibration result may be worse. Based on our research, the market volatility surface must meet at least the following two conditions for a good calibration:

(C1): The variances of ATM volatilities increase with expiration tenors. For example, from Table 2, the 1D ATM volatility is 6.446%, the 1W ATM volatility is 4.2% (since $\text{ExpDate} = 20220930$, it has only 4 days), the 2W ATM volatility is 3.25% (14 days), and so on. Then this condition asks

$$6.446^2 \times 1 \leq 4.2^2 \times 4 \leq 3.25^2 \times 14 \leq \dots \quad (48)$$

(C2): For every expiration tenor, the BF25 volatility is greater than zero and less than the BF10 volatility. For example, for the 1Y tenor in Table 2,

$$\begin{aligned} \text{BF25} &= \frac{1}{2}(4.3238 + 4.7488) - 4.3 = 0.2363, \\ \text{BF10} &= \frac{1}{2}(4.3114 + 5.3114) - 4.3 = 0.5114. \end{aligned} \quad (49)$$

Thus, we have $0 \leq \text{BF25} \leq \text{BF10}$. This condition must also be held for other tenors.

Table 4: Result of Volatility Calibration by LM/Grid Method, AvgError = 0.0003.

Instr	MarketVol	Strike	MarketPrice	ModelPrice	Error
1D_ATM	6.4460	7.09031	95.3935	95.3925	-0.0000
1W_25P	4.2750	7.06759	47.3778	47.3772	-0.0000
1W_ATM	4.2000	7.08888	124.2192	124.2183	-0.0000
1W_25C	4.2750	7.11037	47.1660	47.1644	-0.0000
2W_10P	3.4805	7.02583	22.9127	22.9131	0.0000
2W_25P	3.3375	7.05627	69.2511	69.2514	0.0000
2W_ATM	3.2500	7.08729	179.7794	179.7761	0.0000
2W_25C	3.3775	7.11875	68.7994	68.7923	-0.0001
2W_10C	3.7305	7.15413	24.4149	24.4158	0.0000
3W_10P	3.8281	7.00276	30.8771	30.8800	0.0001
3W_25P	3.6855	7.04349	93.7119	93.7118	-0.0000
3W_ATM	3.5980	7.08533	243.6170	243.6165	-0.0000
3W_25C	3.6855	7.12796	92.8860	92.8874	0.0000
3W_10C	4.0781	7.17502	32.6356	32.6278	-0.0002
1M_10P	4.3355	6.97183	41.8243	41.8281	0.0001
1M_25P	4.1810	7.02688	127.1780	126.9918	-0.0015
1M_ATM	4.0560	7.08319	328.0121	328.0098	-0.0000
1M_25C	4.1810	7.14118	125.6607	125.6466	-0.0001
1M_10C	4.5855	7.20412	43.7688	43.8282	0.0014
2M_10P	4.3397	6.92008	58.6873	58.6866	-0.0000
2M_25P	4.1644	6.99698	177.6282	177.6174	-0.0001
2M_ATM	4.1130	7.07453	465.3075	465.3436	0.0001
2M_25C	4.3144	7.15974	180.9127	180.9211	0.0000
2M_10C	4.6897	7.24970	62.4719	62.4791	0.0001
3M_10P	4.6009	6.86372	77.2500	77.2685	0.0002
3M_25P	4.4779	6.96241	237.2618	237.2635	0.0000
3M_ATM	4.4500	7.06640	623.5861	623.5448	-0.0001
3M_25C	4.7279	7.18178	244.8102	244.8232	0.0001
3M_10C	5.1009	7.30314	83.9403	83.9400	-0.0000
6M_10P	4.5013	6.76477	105.4837	105.4759	-0.0001
6M_25P	4.4060	6.89838	326.0658	326.0686	0.0000
6M_ATM	4.3500	7.04005	847.7307	847.8345	0.0001
6M_25C	4.7560	7.20393	340.8460	340.8558	0.0000
6M_10C	5.2013	7.38124	118.4995	118.5032	0.0000
9M_10P	4.3574	6.69937	125.4967	125.4916	-0.0000
9M_25P	4.3344	6.85521	394.5328	394.4917	-0.0001
9M_ATM	4.3000	7.02575	1027.2206	1027.0325	-0.0002
9M_25C	4.7344	7.22847	414.3587	414.3456	-0.0000
9M_10C	5.2574	7.45485	146.2854	146.2823	-0.0000

Table 4: (Continued)

Instr	MarketVol	Strike	MarketPrice	ModelPrice	Error
1Y_10P	4.3114	6.63663	142.6636	142.7026	0.0003
1Y_25P	4.3238	6.81203	452.4687	452.4639	-0.0000
1Y_ATM	4.3000	7.00700	1177.4686	1177.2818	-0.0002
1Y_25C	4.7488	7.24315	474.8915	474.9302	0.0001
1Y_10C	5.3114	7.51097	168.8805	168.8806	0.0000
18M_10P	4.2841	6.55839	171.9610	171.9223	-0.0002
18M_25P	4.3260	6.76832	549.7037	549.7591	-0.0001
18M_ATM	4.3000	7.00455	1422.6565	1422.3343	-0.0002
18M_25C	4.8010	7.30029	576.9045	577.0090	0.0002
18M_10C	5.3341	7.63197	203.9122	203.9107	-0.0000
2Y_10P	4.2533	6.49377	195.2634	195.2728	0.0000
2Y_25P	4.2909	6.73300	624.0373	624.0487	0.0000
2Y_ATM	4.3000	7.00130	1621.7772	1621.8055	0.0000
2Y_25C	4.8409	7.34925	660.0036	660.0085	0.0000
2Y_10C	5.3533	7.73650	232.3157	232.3095	-0.0000
3Y_10P	4.2536	6.41724	234.7247	234.7244	-0.0000
3Y_25P	4.3420	6.70437	760.3419	760.3198	0.0000
3Y_ATM	4.3000	7.03305	1938.1189	1938.0847	-0.0000
3Y_25C	4.8920	7.47310	790.8628	790.8363	-0.0000
3Y_10C	5.3536	7.95382	275.7694	275.7730	0.0000

7 Pricing precision

Once the volatility calibration is properly done, we can use the local volatility function $\sigma(t, S)$ to construct a pricer and evaluate option deal prices. Although the pricer, whether built using grid or Monte-Carlo methods, can deliver accurate prices for European options, calculation errors are unavoidable when pricing American or Asian options. The following are two examples that demonstrate calculation errors caused by the number of grids (or number of Monte-Carlo paths) used in pricing.

Table 5 shows the values of four American option deals calculated using the grid method with varying numbers of half-grids. The 1Y_ATM deal is an extension of the 1-year ATM European option instrument in Table 4, and the same applies to the other three deals. The grid method was used to price these four American options, with half-grid numbers I of 50,

Table 5: The Effect of Grid Number on American Options. Pricing Date: 20220926.

Deal	1Y_ATM	1Y_10C	6M_ATM	1M_ATM
I=50	1290.4302	173.9357	920.4592	331.7334
I=100	1290.1247	173.9330	920.2302	331.7870
I=200	1290.2568	173.9315	920.1014	331.8036
Strike	7.00700	7.51097	7.04005	7.08319
ExpDate	20230926	20030926	20030324	20021026
PayDate	20230928	20030928	20030328	20021028
EuroPrc	1177.4686	168.8805	847.7307	328.0121

100, and 200. The pricing values are listed in the table. The results demonstrate that the grid method is highly stable, with calculation results for a given deal differing by no more than 1 basis point across different values of I .

Table 6: The Effect of Path Number on Asian Options. Pricing Date: 20220926.

Deal	1Y_ATM	1Y_10C	6M_ATM	1M_ATM
I=5000	883.2436	11.8253	608.9964	186.5733
I=10000	881.1290	12.0545	612.8797	186.9654
I=15000	878.8648	11.9601	612.0276	186.9369
I=20000	881.0790	12.6660	611.2084	187.3059
Strike	7.00700	7.51097	7.04005	7.08319
LastFix	20230926	20030926	20030324	20021026
PayDate	20230928	20030928	20030328	20021028
EuroPrc	1177.4686	168.8805	847.7307	328.0121

Table 6 shows the values of four Asian option deals calculated using the Monte-Carlo method with different numbers of paths, I . Each deal was constructed from the extension of the European option instrument of the same name in Table 4. For all four deals, the FX fixing dates were set to Fridays, or the following CFETS business day if Friday is a holiday. The numbers of paths I were taken as 5000, 10000, 15000, and 20000, respectively. From the table, we see that for short-term deals such as 1M_ATM and out-of-the-money deals like 1Y_10C, the prices are stable within 1 basis point. Even for the long-term deal like 1Y_ATM, there is only about a 2 basis point variation in the prices, which basically satisfies

the business requirements. Moreover, to further improve pricing precision, we can increase the number of paths I , increase the number of local volatility grids (currently 18×11), or increase the number of time steps.

8 Local-stochastic volatility model

The local volatility model (LV), proposed in this paper, can be easily extended to the local-stochastic volatility model (LSV). For example, if the Heston model is used to formulate the stochastic volatility feature, the underlying FX rate S and its variance rate V are driven by two correlated Brownian motions, namely, w_1 and w_2 ,

$$\begin{aligned}\frac{dS}{S} &= \sigma(t, S)\sqrt{V}dw_1, \\ dV &= \kappa(\theta - V)dt + \varepsilon\sqrt{V}dw_2, \\ dw_1 \cdot dw_2 &= \rho dt.\end{aligned}\tag{50}$$

where, κ , θ , ε , ρ , $V_0 = V(0)$ (not shown in the formulas) are the five free parameters of the Heston model.

In the history of model development, a major objective of LSV has been to have more free model parameters in order to calibrate the strong market volatility skew, which is shown in Table 2, for example. There have been many achievements in LSV research, as seen in references [1-7]. Based on these references and our work in this paper, we would like to make two comments. Firstly, the LSV is a two-factor model which requires a two-dimensional grid or Monte-Carlo numerical method. The coding complexity and computation time will increase to a multiple level compared to the current LV model. Secondly, no matter how the local volatility function $\sigma(t, S)$ is selected, volatility calibrations always yield poor results if there are not enough free parameters to support it. For instance, [7] presents a scenario in which 30 free parameters are chosen in $\sigma(t, S)$ to calibrate 30 volatility instruments, and the AvgError is 0.0177. Clearly, this result falls short of meeting the requirements of trading businesses.

The fully parameterized one-factor local volatility model proposed in this paper can be accurately and efficiently calibrated to the volatility skew, which meets the requirements of

our trading desk. Therefore, there is no need to extend this model to the two-dimensional LSV model.

Acknowledgement: We would like to express our sincere thanks to our colleagues CHEN Xuejun, WEN Yang, and LI Yipeng from the FX trading division of CCB Financial Market Department for their significant contributions in developing, validating, and working with the LV model in this paper. We could not have achieved success without their support.

Reference

1. C. Homescu: Local stochastic volatility models: calibration and pricing. <http://www.researchgate.net/publication/272247504>, (2014).
2. E. Derman and I. Kani: Stochastic implied trees: arbitrage pricing with stochastic term and strike structure of volatility. *Goldman Sachs Quantitative Strategies Research Notes*, <http://www.researchgate.net/publication/240264588>, (1997).
3. S.L. Heston: A closed-form solution for options with stochastic volatility with applications to bond and currency options. *The Review of Financial Studies*, 6 327-343 (1993).
4. L. Andersen: Simple and efficient simulation of the Heston stochastic volatility model. *Journal of Computational Finance*, 11(3) 1-42 (2008).
5. A. van der Stoep, L.A. Grzelak, C.W. Oosterlee: The Heston Stochastic-Local Volatility Model: Efficient Monte Carlo Simulation, *International Journal of Theoretical and Applied Finance*, 17(7) (2014).
6. U.P. Wystup: The Tremor Model The Tremor Stochastic-Local-Volatility Model Independent Validation by MathFinance. <http://researchgate.net/publication/265408143>.
7. X. Lin: The Pricing Models for CNY Structured Deposit Trades (in Chinese), (2019). <http://www.researchgate.net/publication/336275297>.

8. X. Lin and J. Ballmann: A Riemann solver and a second-order Godunov method for elastic-plastic wave propagation in solids, *International Journal of Impact Engineering*, 13(3) 463-478 (1993). <http://www.researchgate.net/publication/245148831>.